Eur J Nutr (2016) 55:997–1010
DOI 10.1007/s00394-015-0914-1

ORIGINAL CONTRIBUTION

Multiplatform metabolomic fingerprinting as a tool for understanding hypercholesterolemia in Wistar rats

Diana González-Peña[1] · Danuta Dudzik[2] · Clara Colina-Coca[1] · Begoña de Ancos[1] · Antonia García[2] · Coral Barbas[2] · Concepción Sánchez-Moreno[1]

Received: 3 December 2014 / Accepted: 25 April 2015 / Published online: 13 May 2015
© Springer-Verlag Berlin Heidelberg 2015

Abstract
Purpose The aim was to investigate the impact of hypercholesterolemic diet on the metabolome of male Wistar rats by a multiplatform metabolomic fingerprinting.
Methods Male Wistar rats were fed with two different diets [control (C) and high-cholesterol diet (HC)—containing 2 % cholesterol and 0.5 % cholic acid]. After 7 weeks of experimental feeding, the rats were euthanized for blood collection and plasma recovery. The metabolite fingerprint was then achieved by applying a multiplatform comprising LC–MS, GC–MS and CE–MS.
Results Multivariate statistical analysis showed a clear separation between the C and HC groups. Individual differences in metabolites were evaluated using univariate statistical analysis, and multiple metabolites were identified and confirmed in the plasma. A global profiling integrates for the first time pathways affected by high-cholesterol diet intake and allowed us to elucidate some of the associated alterations underlying the hypercholesterolemia event in Wistar rats.
Conclusions HC feeding stimulated the alteration of multiple pathways in Wistar rats, warning of the risk of developing important diseases, which can be modulated by the diet. Further studies are required to investigate the possibilities to revert or ameliorate the negative effects triggered by HC intake.

✉ Concepción Sánchez-Moreno
csanchezm@ictan.csic.es

[1] Institute of Food Science, Technology and Nutrition (ICTAN), Spanish National Research Council (CSIC), José Antonio Novais 10, 28040 Madrid, Spain

[2] Center for Metabolomics and Bioanalysis (CEMBIO), Faculty of Pharmacy, San Pablo CEU University, Boadilla del Monte, 28668 Madrid, Spain

Keywords Atherosclerosis · Global profiling · High-cholesterol diet · Metabolomics · Untargeted analysis

Introduction

Although coronary heart disease mortality rates have decreased during the last decades in the majority of the European countries, cardiovascular disease (CVD) stays as one of the main causes of mortality, with more than four millions of deaths per year [1]. Multiple actions for its prevention (mainly involving changes in lifestyle and nutritional status) have been pointed out in the literature for evidencing a clear association between hypercaloric diets, overweight and obesity, and a high risk of developing metabolic and cardiovascular disorders [2–6]. In this sense, the consumption of a diet with a high content of high saturated fatty acids and cholesterol has been highlighted as accelerators in the progression of CVD, playing also a key role in the initial stages of atherosclerosis [7–9].

Animal studies are biological tools extendedly used to get knowledge on nutrient–metabolism interactions. They are considered free of interferences caused by several environmental factors (such as exposure to contaminants, medications, clime, physical activity and diversity of diet), thus providing a valuable source of information for the interpretation of mechanisms of action and pathways involved in numerous diseases [10]. Accordingly, the effects of phytochemicals, nutraceuticals and diverse dietary intakes on hypercholesterolemia and obesity have been evaluated in animal models, along with the evaluation of the different pros and cons of each one in specific functions, by means of different platforms [11–15]. Nevertheless, none of those variations were reached beyond a deeply studied system,

whose changes in metabolome had been described working as a whole into a comprehensive model of hypercholesterolemia induced by diet, by means of multiple approaches performed simultaneously.

To achieve this goal, metabolomics and its combination with sensitive analytical techniques and univariate/multivariate statistical analysis arise as an innovative and fast approach to investigate changes in metabolism. In this trend, metabolic fingerprinting may be highlighted and described as an approach that looks for a total profile (also called fingerprint) as a unique pattern capable to characterize metabolism in a particular case [16], being clearly of relevance for the study of diet-related diseases [17]. Metabolomics improves the understanding of the effects of certain diets or foodstuffs on metabolic pathways and the relationship between dietary habits and chronic diseases [18]. The characterization of the metabolome of an hypercholesterolemic model may not only help to understand fundamental biochemistry that gives further insights into the pathophysiological mechanisms involved in a particular disease, but also it is a valuable tool for the identification of biomarkers. Furthermore, it could be used for early diagnosis, monitoring disease progression [19] as well as showing responses and treatment effects of nutritional interventions.

In the present work, an analytical multiplatform for metabolomics of hypercholesterolemia as a diet-related disease has been successfully applied, including liquid chromatography, gas chromatography and capillary electrophoresis techniques coupled to mass spectrometry, as fingerprinting approaches, to study the impact of cholesterol supplementation within the diet on the metabolome of male Wistar rats.

Materials and methods

Animals and diets

The study was performed in compliance with the Directive 2010/63/UE regarding the protection of animals used for scientific purposes and was approved by the Spanish Ministry of Science and Innovation Advisory Committee [Project AGL2010-15910 (subprogram ALI)] and by an Ethics Committee of the Complutense University of Madrid (Spain).

Male Wistar rats with a body weight of 245 ± 5 g ($n = 16$) were obtained from Harlan Laboratories Models (Harlan, SL, Barcelona, Spain) and randomly divided into two experimental groups. The animals were placed in individual metabolic cages under controlled conditions of light (12-h light/dark cycle) and temperature (22 ± 1 °C). All rats were given free access to diet and water but fed accordingly to either a control (C) diet composed of a homogeneous mixture of 100 % rodent diet or a high-cholesterol (HC) diet containing 2 % cholesterol and 0.5 % cholic acid, substituting an equal amount of maize starch. The nutritional composition of the diets is detailed in Table 1. The experimental period was extended for 7 weeks, recording body weight and food consumption (after 1-week acclimatization for the progressive adaptation to environmental conditions, housing and control diet).

Blood collection and sample preparation

Animals were maintained 2 h in fasting conditions prior deep inhalation of isoflurane anesthesia and death by exsanguination. Blood samples were collected by cardiac

Table 1 Composition of the control (C) and high-cholesterol (HC) diets

Ingredient (g/kg)[c]	C	HC
Casein	200	200
Sucrose	100	100
Maize starch	470.49	445.49
Soya oil	50	50
Maize oil	80	80
Mineral mixture[a]	35	35
Vitamin mixture[b]	10	10
Cellulose powder	50	50
Choline bitartrate	2.5	2.5
tert-butylhydroquinone	0.010	0.010
L-Cystine	2	2
Cholesterol	–	20
Cholic acid	–	5

C control, *HC* high-cholesterol

[a] Mineral mix for the AIN-93M diet, g/kg: calcium carbonate anhydrous, 357.00; potassium phosphate monobasic, 250.00; potassium citrate, tripotassium monohydrate, 28.00; sodium chloride, 74.00; potassium sulfate, 46.00; magnesium oxide, 24.00; ferric citrate, 6.06; zinc carbonate, 1.65; sodium meta-silicate $9H_2O$, 1.45; manganous carbonate, 0.63; cupric carbonate, 0.30; chromium potassium sulfate $12H_2O$, 0.275; boric acid, 0.0815; sodium fluoride, 0.0635; nickel carbonate, 0.0318; lithium chloride, 0.0174; sodium selenate anhydrous, 0.01025; potassium iodate, 0.0100; ammonium paramolybdate $4H_2O$, 0.00795; ammonium vanadate, 0.0066; powdered sucrose, 209.806

[b] AIN-93-VX vitamin mix for the AIN-93M diet, g/kg: niacin, 3.000; calcium pantothenate, 1.600; pyridoxine–HCl, 0.700; thiamin-HCl, 0.600; riboflavin, 0.600; folic acid, 0.200; biotin, 0.200; vitamin B_{12} (0.1 %), 2.500; vitamin E (all-*rac*-α-tocopheryl acetate, 500 IU/g), 15.000; vitamin A (all-*trans*-retinyl palmitate, 500,000 IU/g), 0.800; vitamin D3 (400,000 IU/g), 0.250; vitamin K1, 0.075; powdered sucrose, 974.655

[c] Diet energy content was calculated using the factors 16.73 kJ/g (4 kcal/g) for protein, 15.69 kJ/g (3.75 kcal/g) for monosaccharides, 16.53 kJ/g (3.95 kcal/g) for disaccharides, 17.49 kJ/g (4.18 kcal/g) for starch, 8.37 kJ/g (2 kcal/g) for dietary fiber, and 37.65 kJ/g for fat. Control diet, 18,540.9 kJ/kg (4431.4 kcal/kg); HC diet, 18,856.6 kJ/kg (4506.8 kcal/kg)

puncture of the right ventricle in BD Vacutainer® tubes containing EDTA as anticoagulant and were immediately centrifuged at 1500×*g* for 15 min at 4 °C to obtain plasma. Aliquots of the recovered plasma were stored at −80 °C until analysis in three different fingerprinting platforms. For each platform, frozen plasma samples were thawed on ice and subsequently mixed using vortex before sample preparation procedure.

LC–MS

Plasma deproteinization and metabolite extraction were performed with cold mixture of methanol/ethanol followed by centrifugation at 16,000×*g* for 10 min at 4 °C (centrifuge 5415 R Eppendorf). The supernatant was filtered using a 0.22-µm nylon filter to LC/MS vials [20].

GC–MS

Plasma deproteinization was performed with cold acetonitrile followed by centrifugation at 15,400×*g* for 10 min at 4 °C (5415 R Eppendorf). In total, 100 µL of the supernatant was transferred into a GC vial and evaporated to dryness at 35 °C by SpeedVac SPD121P (Thermo Fisher Scientific, Waltham, MA.). For methoximation, 10 µL of *O*-methoxyamine hydrochloride (15 mg/mL) in pyridine was added to each GC vial and vortexed. The vials were incubated in darkness at room temperature for 16 h. After adding 10 µL of BSTFA with 1 % TMCS (v/v), the samples were vortexed for 5 min and then incubated at 70 °C for 1 h for silylation reaction. At the end of procedure, 100 µL of internal standard C18:0 methyl ester (10 mg/mL in heptane) was added to each GC vial. Three blank samples were prepared by following the same procedure of extraction and derivatization. Blank samples were analyzed at the beginning, in the middle and at the end of the sequence [21].

CE–MS

Each plasma sample (100 µL) was mixed with 100 µL 0.2 M formic acid (with 5 % acetonitrile and 0.4 mM methionine sulfone as internal standard). Sample was vortex-mixed for approximately 1 min and then transferred to a Centrifree Millipore (30 kDa) filter and centrifuge (2000×*g*, 70 min, 4 °C). The supernatant was then transferred directly to a vial for analysis [22].

Quality control (QC)

QC samples were prepared by pooling equal volumes of each plasma sample following the same procedure as for sample preparation and were injected at the beginning/end, and every six samples injections, of each analysis. QC samples were analyzed throughout the run to provide a measurement of the system's stability and performance as well as reproducibility of the sample preparation procedure [23].

Metabolic fingerprinting

Instrumentations and conditions

LC–QTOF–MS Liquid chromatography–quadrupole time of flight–mass spectrometry. The experiments were performed using an UHPLC system (Agilent 1290 Infinity LC System) composed of a degasser, two binary pumps and a thermostated autosampler (maintained at 4 °C) coupled with Q-TOF LC/MS (6550 iFunnel) system (Agilent Technologies). In total, 0.5 µL of extracted plasma samples was injected to a reverse-phase Zorbax Extend C_{18} column (2.1 × 50 mm, 1.8 µm; Agilent Technologies) thermostated at 60 °C. The flow rate of mobile phase (A: water with 0.1 % formic acid and B: acetonitrile with 0.1 % formic acid) was 0.6 mL/min running in gradient method from 5 to 100 % B phase. During all analyses, two reference masses were used: *m/z* 121.0509 ($C_5H_4N_4$) and *m/z* 922.0098 ($C_{18}H_{18}O_6N_3P_3F_{24}$) for positive ionization mode (ESI+) and *m/z* 112.9856 [$C_2O_2F_3$ (NH_4)] and *m/z* 1033.9881 ($C_{18}H_{18}O_6N_3P_3F_{24}$) for negative ionization mode (ESI−), continuously infused into the system for constant mass correction. The system was operated in full scan mode from 50 to 1000 *m/z* for positive and 50 to 1100 *m/z* for negative modes. Capillary voltage was set to 3 kV for both positive and negative ionization modes; the drying gas flow rate was 12 L/min at 250 °C and gas nebulizer 52 psi, fragmentor voltage 175 V for positive and 250 V for negative ionization modes, skimmer 65 V and octopole radio frequency voltage (OCT RF Vpp) 750 V. Data were collected in the centroid mode at a scan rate of 1.0 spectrum per second.

GC–EI–Q–MS Gas chromatography–electron impact–single quadrupole–mass spectrometry. GC system (Agilent Technologies 7890A) consisted in an autosampler (Agilent Technologies 7693) interfaced to inert mass spectrometer with triple-Axis detector (5975C, Agilent Technologies). In total 2 µL of the derivatized sample was injected through a GC-Column DB5-MS (30 m length, 0.25 mm, 0.25 µm film 95 % dimethyl/5 % diphenylpolysiloxane) with a pre-column (10 m J&W integrated with Agilent 122-5532G). The injector port was held at 250 °C, and the split ratio was 1:10 with helium carrier gas flow rate 1.0 mL/min. The temperature gradient was programmed as follows: The initial oven temperature was set at 60 °C (held for 1 min), increased to 325 °C at 10 °C/min rate, a cooldown period was applied for 10 min before the next

injection. Retention time locking tool was used during the analysis. The detector transfer line, the filament source and the quadrupole temperature were, respectively, set at 280, 230 and 150 °C. MS detection was performed with electron impact (EI) mode at−70 eV. The mass spectrometer operated in scan mode over a mass range of 50–600 *m/z* at a rate of 2.7 scan/s. All these conditions were previously optimized [24].

CE–TOF–MS Capillary electrophoresis–time of flight–mass spectrometry. Agilent 7100 Capillary Electrophoresis system coupled with a TOF mass spectrometer (6224 Agilent) was used for sample analysis. The coupling was equipped with an electrospray ionization source. A 1200 series ISO Pump from Agilent Technologies was used to supply sheath liquid. The separation occurred in a fused-silica capillary (Agilent Technologies) with a diameter of 50 μm and length 96 cm. New capillaries were preconditioned with flush of: 1 M NaOH for 30 min followed by MilliQ® water for 30 min and background electrolyte—BGE (0.8 M formic acid in 10 % methanol) for 30 min. Before each analysis, the capillary was flushed for 5 min (950 mbar pressure) with BGE. Samples were injected at 50 mbar pressure for 50 s. After each sample injection, the BGE was injected for 20 s at 100 mbar pressure to improve the reproducibility. The separation conditions included 25 mbar of pressure and 30 kV of voltage. The current observed under these conditions was 20 μA. Before each injection, the instrument automatically replaced the BGE. The MS was operated in positive polarity. Drying gas was set to 10 L/min, nebulizer 10 psi, voltage 3.5 kV, fragmentor 100 V, gas temperature 200 °C and skimmer 65 V. The sheath liquid composition was methanol/water (1/1, v/v) containing 1.0 mmol/L formic acid with two reference standards: standards (10 μL of 5 mM $C_5H_4N_4$, *m/z*—121.0509 + 30 μL of 2.5 mM $C_{18}H_{18}O_6N_3P_3F_{24}$, *m/z*—922.0098), using a flow rate of 0.6 mL/min (split 1/100). For MS, the total separation time (35 min) was divided into two segments; the first segment was for 1 min without applying nebulization and the remaining 34 min with nebulization. The conditions for the separation CE and detection in MS were optimized from a previously developed method in our laboratory [22].

Data acquisition and statistical analysis

Raw data acquired using LC–MS, GC–MS and CE–MS were processed to provide structured data in an appropriate format for data analysis. The raw data collected by LC–MS and CE–MS were cleaned of background noises, and unrelated ions by the molecular feature extraction (MFE) tool in the MassHunter Qualitative Analysis Software (B.05.00, Agilent Technologies).

For GC–MS data, corresponding peak detection and spectra processing were obtained using Agilent ChemStation software (G1701EA E.02.00.493, Agilent). Automated Mass Spectral Deconvolution and Identification System (AMDIS) version 2.69 software from US National Institute of Standards and Technology (NIST) was used for mass spectral deconvolution to identify co-eluted compounds according to their retention indexes and retention times. GC–MS data were normalized according to C18:0 methyl ester intensity.

Primary data treatment, alignment of drift (by retention time and mass) and data filtering were performed with Mass Profiler Professional B.12.1 (Agilent Technologies) and Excel (Microsoft Office 2013) software. To keep only metabolites with a good repeatability, only features with RSD <30 % in QC were evaluated as relevant.

Data matrix was exported into SIMCA-P+ 12.0 (Umetrics, Umeå, Sweden) for multivariate (unsupervised and supervised) statistical analysis, multivariate calculation as well as visualization procedures. Differences between control and HC groups for LC–MS and CE–MS analysis were evaluated for individual metabolites using univariate statistical analysis (*t* test) assuming unequal variance (Welch's *t* test) performed with Mass Profiler Professional B.12.1 (Agilent Technologies). A p value <0.05 was considered significant to select metabolites and was calculated for data transformed by applying a log (base 2) for intensities in order to approximate a normal distribution. A Benjamin Hochberg FDR correction was also applied to adjust the p values. In multivariate analysis, variable selection was performed by applying a confidence interval based on a *Jack–Knife* procedure (Umetrics, Umeå, Sweden) and using an in-house script developed at Matlab R2010a (Mathworks) software (for GC–MS).

Compound identification

Accurate masses of features representing significant differences in class separation identified by LC–MS and CE–MS approach were searched against the online available databases METLIN (http://metlin.scripps.edu), KEGG (http://genome.jp/kegg) and LIPIDMAPS (http://lipidmaps.org) by the in-house developed CEU mass mediator (http://ceu-mass.eps.uspceu.es/mediator) and HMDB (http://hmdb.ca). The identity of compounds was confirmed by LC–MS/MS by using a QTOF (6550 system, Agilent Technologies) with the same chromatographic conditions as applied for the primary analysis. Ions were targeted by collision-induced dissociation (CID) fragmentation on the fly based on the previously determined accurate mass and retention time. Accurate mass and isotopic distributions for the precursor and product ion have been studied for confirmation of the particular compounds. For CE–MS data, the identification

of compounds was confirmed by injecting available standards, plasma samples and spiked plasma samples for its comparison.

Compound identification by GC–MS was performed by using the target metabolite Fiehn GC/MS Metabolomics RTL (Retention Time Locked) library (G1676AA, Agilent Technologies), the in-house CEMBIO library and the NIST mass spectra library 2.0, with the ChemStation software and native probability-based matching (PBM) algorithm (G1701EA E.02.00.493, Agilent). Compound identification includes retention index (RI) and the retention time (RT) information. The identification is assured by the reproducibility of EI mass spectra and RTL method (according to the Internal Standard—C18:0 methyl ester).

Experiment validation

OPLS/O2PLS-DA models obtained according to multivariate calculations were validated by using of a cross-validation tool, which has been described elsewhere [25]. Briefly reviewed, a randomized data set was divided into three parts and one-third of samples were excluded to build a model with the remaining two-third of samples. Then, excluded samples were predicted by the new model, repeating the process until all samples were predicted at least once. Each time the percentage of correctly classified samples was calculated.

Results

Animal growth was followed up during the whole experiment under strict control, verifying a regular daily intake of diets and water, urine and fecal excretion and behavior of each individual rat in the study. Finally, the statistical trend of weekly food intake and the curves for weight gain were plot (Fig. 1). Food intake, body weight gain (g) and food efficiency ratio (FER) were calculated showing no statistical differences between the HC and C groups. On the other hand, fecal weight (g/d) mean value evidenced an increase in HC-fed group. Apparent diet digestibility was higher than 99.6 % (dry matter) in all cases, but dietary cholesterol supplementation decreased it significantly in HC-fed group (Table 2).

The metabolite fingerprint was then achieved by applying a multiplatform LC–MS, GC–MS and CE–MS approach to plasma collected the day of sacrifice. Data matrices obtained after peak alignment and filtering were used for multivariate unsupervised principal component analysis (PCA) to check the distribution of QC samples of each technique. The QC samples were clustering together in all cases, reflecting the system's stability, performance and reproducibility of the sample treatment procedures [23]. Variation of the compound concentrations in QC samples expressed as relative standard deviation (% RSD) was also calculated.

Data sets after alignment and filtering, counting with 1037 entities in LC–MS positive ionization mode, 220 entities in LC–MS negative ionization mode and 432 entities in CE–MS and 56 identified compounds in GC–MS, were firstly used to conduct PCA unsupervised analysis to investigate whether there was an apparent metabolomics separation between plasma from control and hypercholesterolemic

Table 2 Food intake, initial body weight, final body weight, body weight gain, dietary efficiency ratio, food efficiency ratio, fecal weight and apparent diet digestibility in rats fed the control (C) and high-cholesterol (HC) diets for 7 weeks

	C	HC
Food intake (g/day/rat)	16.14 ± 0.20	15.99 ± 0.18
Body weight gain (g)	141.80 ± 9.75	133.68 ± 6.93
Food efficiency ratio[a]	19.56 ± 1.26	18.30 ± 0.48
Fecal weight (g fresh matter/day)	2.22 ± 0.07	4.25 ± 0.06*
Apparent diet digestibility (% dry matter)[b]	99.81 ± 0.008	99.64 ± 0.012*

The data are presented as the mean ± SE ($n = 8$ per group)

C control, *HC* high-cholesterol

* ($p < 0.05$) indicates a significant difference between the control and the HC-fed groups (Student's *t* test)

[a] 100 × (body weight gain/total food intake)

[b] 100 × (total food intake− fecal weight/food intake)

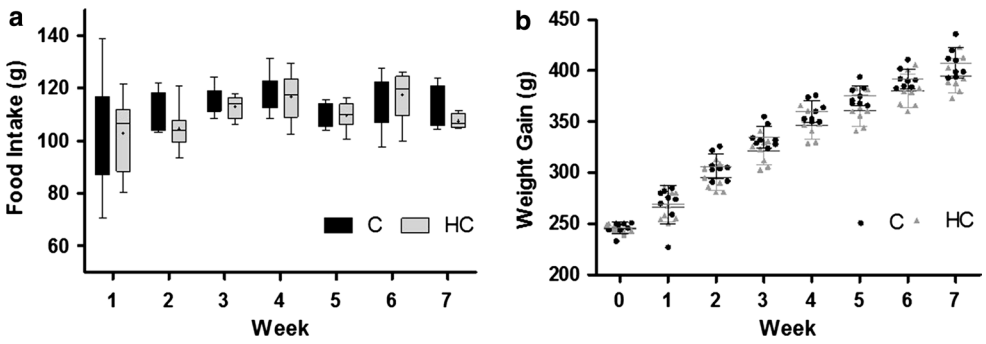


Fig. 1 Food intake (**a**) and growth curve (**b**) of rats fed control diet or cholesterol-rich diet for 7 weeks. *C* control diet (*filled circles*), *HC* high-cholesterol diet (*filled triangles*)

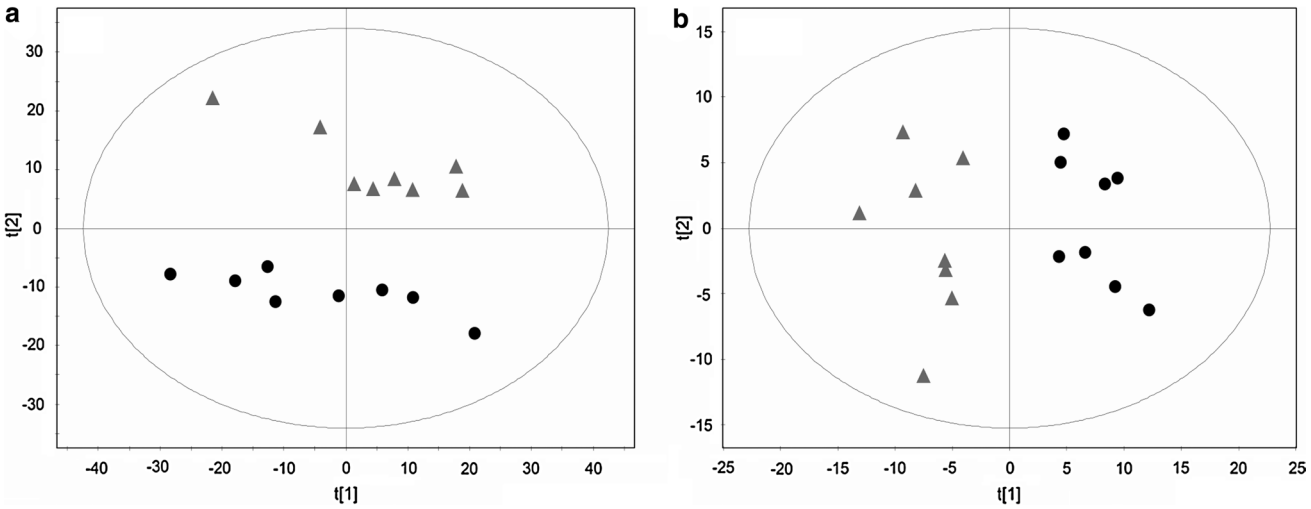


Fig. 2 Score plots of control (*filled circles*) and high-cholesterol fed group (*filled triangles*) unsupervised PCA-X analysis. **a** LC–MS ESI+ ($R^2 = 0.35$, $Q^2 = 0.11$) and **b** LC–MS ESI− ($R^2 = 0.042$, $Q^2 = 0.16$)

rats. In particular, as it may be noticed in Fig. 2, clear separation for LC–MS data was observed between the two groups, indicating that inherent metabolic changes occur under hypercholesterolemic condition. Additionally, supervised partial least squares discriminant analysis (PLS-DA) and orthogonal PLS (OPLS-DA) discriminant analysis were used for modeling the differences between HC and C groups. Multivariate models showed a clear separation of samples as it may be confirmed by the good quality of the OPLS-DA models (Fig. 3): explained variance $R^2 = 0.99$ (LC–MS ESI+), $R^2 = 0.98$ (LC–MS ESI–), $R^2 = 0.97$ (GC–MS) and $R^2 = 0.99$ (CE–MS) and predicted variance $Q^2 = 0.83$ (LC–MS ESI+), $Q^2 = 0.91$ (LC–MS ESI–), $Q^2 = 0.70$ (GC–MS) and $Q^2 = 0.53$ (CE–MS). The predictive ability of the OPLS-DA models was estimated by the cross-validation tool described in "Experiment validation" section. Data recorded for LC–MS showed how all excluded samples were correctly classified in 91 and 94 % of cases, in LC–MS ESI+ mode and ESI− mode, respectively. However, validation for GC–MS of analyzed samples evidenced 86 % of success, while in CE–MS only 52 % of all samples were classified correctly, which means that stronger classifiers can be obtained from LC–MS and GC–MS than from CE–MS. Parallel to these analyses, the univariate statistical interpretation revealed individual significant metabolites, which were compared in each applied technique yielding: 200 statistically significant features in LC–MS ESI+, 101 in LC–MS ESI−, 13 in GC–MS and 57 in CE–MS. Identification of those metabolites was performed as described in "Compound identification" section, including the calculation of mass error of measured mass in comparison with monoisotopic mass from databases (except for those analyzed by GC–MS). Benjamin Hochberg FDR correction was applied; however, some metabolites fitting the proper change in the corresponding metabolic pathways were kept even when they did not pass this restrictive correction for improved information. Final identified metabolites from each technique are summarized in Tables 3, 4 and 5 incorporating information relative to retention time, the monoisotopic mass, percentage of changes between groups and statistical significance, among others.

Discussion

The role of metabolomics in the field of nutrition is growing markedly as its utility to elucidate metabolic alterations, mechanisms of action involved in pathological processes and new health/disease biomarkers, or dietary intake biomarkers has been widely demonstrated [17, 18, 26, 27]. The combination of different and complementary analytical platforms as LC–QTOF–MS, GC–Q–MS and CE–TOF–MS has resulted to be a value and an advantage of the present study. The chemical diversity of the metabolites in addition to a large dynamic concentration range evidenced that more than a unique high-throughput approach is necessary to obtain complete metabolite coverage.

In the present study, the effects of a hypercholesterolemic and potentially atherosclerotic diet—containing 2 % of cholesterol and 0.5 % of cholic acid—were investigated in an animal model (8-week-old male Wistar rats). A list of changes occurring in the Wistar rat metabolome under these specific circumstances has been obtained, describing the deviations produced in their plasma fingerprint after 7 weeks of HC feeding compared to the control. The information achieved provides a preliminary set of

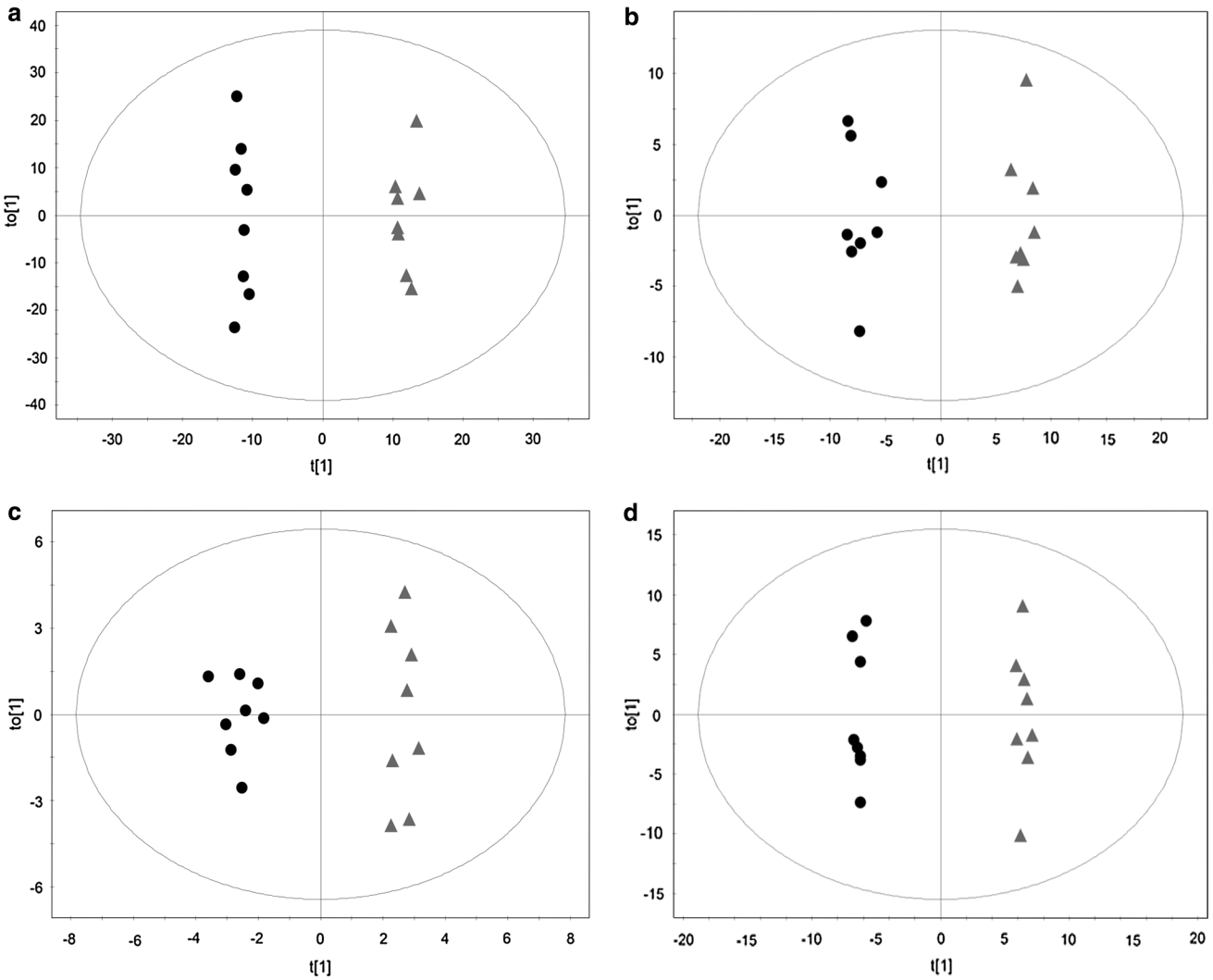


Fig. 3 OPLS-DA plots of plasma metabolic profiles obtained for control and hypercholesterolemic groups. **a**, **b** show OPLS-DA model ($R^2 = 0.99$, $Q^2 = 0.83$ and $R^2 = 0.98$, $Q^2 = 0.91$) (*filled circles* control and *filled triangles* high-cholesterol fed group) based on 1037 LC–MS ESI+ and 220 LC–MS ESI− detected variables. C and D show OPLS-DA model (*filled circles* control and *filled triangles* high-cholesterol fed group) for GC–MS data ($R^2 = 0.97$, $Q^2 = 0.7$) and CE–MS ($R^2 = 0.99$, $Q^2 = 0.53$) based on 56 and 432 detected variables, respectively

metabolites, evidencing some alterations derived from the HC feeding and pointing out some key-affected metabolites whose monitoring could contribute to the prevention of certain diseases. This approach highlights the main pathways involved in hypercholesterolemia, allowing to create hypotheses for future studies, including the evaluation of enzymes and quantification of downstream metabolites in specific metabolic pathways to elucidate the mechanisms of action.

A high-cholesterol intake has been associated with a major risk of type 2 diabetes [28], and it has been considered as a critical cause of nonalcoholic fatty liver disease (NAFLD) [29], regardless of the obesity status. Likewise, increased levels of the markers of cholesterol absorption have been related to a major risk of coronary artery disease for most of the studies recorded to date [30]. The influence of HC diets on the lipid metabolism is primarily known through the alteration of plasma lipid levels together with an increase in the cholesterol forms [31]. The confirmation of this initial condition in this study (data shown in Table 6) added some insights about the presence of certain disorders in the lipid metabolism, which were confirmed by the consequent metabolic fingerprinting analysis performed. This fingerprint might be linked to the initial development of pathological conditions within inflammation, atherosclerosis, and diabetes, among others. To avoid biases in the results, the animal dietary intake, their body weight and the weight of fecal deposits were recorded (Table 2;

Table 3 Differences in plasma metabolites based on LC–MS related to high-cholesterol diet (p value <0.05)

Name	Compound	Mass (DB)	RT (min)	Mass error (ppm)	DET	Change (%)	p value
Fatty acyls							
Arachidonic Acid	$C_{20}H_{32}O_2$	304.2402	6.94	−1.6	ESI−	−46.42	0.015[a]
Glycerophospholipids							
PE (P-19:1)	$C_{24}H_{48}NO_6P$	477.3219	5.58	−1.26	ESI+	−21.36	0.019
PE-NMe2 (16:0/20:4)	$C_{43}H_{78}NO_8P$	767.5465	9.55	−1.4	ESI−	−28.51	0.045[a]
PE (O-36:4) or PE (P-36:3)	$C_{41}H_{76}NO_7P$	725.5359	10.30	−1.32	ESI+	+28.41	0.035
PE (P-38:6)	$C_{43}H_{74}NO_7P$	747.5203	9.71	6.96	ESI+	−55.71	0.033[a]
PC (15:0)	$C_{23}H_{48}NO_7P$	481.3168	5.53	−8	ESI−	−18.22	0.022[a]
PC (18:1/16:0)	$C_{42}H_{82}NO_8P$	760.0761	11.89	0	ESI−	+55.22	0.0087
PC (34:4)	$C_{42}H_{76}NO_8P$	753.5309	8.83	−0.13	ESI+	−29.04	0.032
PC (35:2)	$C_{43}H_{82}NO_8P$	771.5778	11.88	−1.04	ESI+	+64.40	0.012[a]
PC (20:4/16:0)	$C_{44}H_{80}NO_8P$	782.0816	9.55	1	ESI –	−30.82	0.013
PC (36:4)	$C_{44}H_{80}NO_8P$	781.5621	9.66	3.12	ESI+	−43.91	0.026[a]
PC (37:4)	$C_{45}H_{82}NO_8P$	795.5778	10.14	−0.50	ESI+	−53.90	0.0035[a]
PC (20:4/18:0)	$C_{46}H_{84}NO_8P$	809.5935	11.89	3.34	ESI±	−62.48	0.0031[a]
PC (18:2/20:4)	$C_{46}H_{80}NO_8P$	805.5621	9.03	1	ESI±	−39.17	0.0038
PC (18:2/20:4)	$C_{46}H_{80}NO_8P$	805.5622	9.35	1	ESI ±	−71.95	0.0044[a]
PC (40:5)	$C_{48}H_{86}NO_8P$	835.6091	11.87	−144	ESI+	−59.49	0.014[a]
PC (40:7)	$C_{48}H_{82}NO_8P$	831.5778	9.53	00	ESI+	−54.40	0.010[a]
PC (40:8)	$C_{48}H_{80}NO_8P$	829.5621	8.90	0.89	ESI+	−74.80	0.0021[a]
PC (42:10)	$C_{50}H_{80}NO_8P$	853.5622	8.79	0.23	ESI+	−79.79	0.0059[a]
LPE (16:0)	$C_{21}H_{44}NO_7P$	453.2855	5.49	−13	ESI−	+38.04	0.0016[a]
LPE(18:0)	$C_{23}H_{48}O_7P$	481.3168	6.10	−12	ESI−	+41.57	0.028[a]
LPE (18:1)	$C_{23}H_{46}NO_7P$	479.3012	5.65	−14	ESI−	+82.63	0.00009[a]
LPE (18:2)	$C_{23}H_{44}NO_7P$	477.2855	5.29	−1.3	ESI−	+70.61	0.0024[a]
LPC (15:0) sn-1	$C_{23}H_{48}NO_7P$	481.3168	5.28	−0.69	ESI+	+81.59	0.0034[a]
LPC (16:0)	$C_{24}H_{50}NO_7$	495.3325	5.53	4	ESI−	−14.76	0.012
LPC (17:0)	$C_{25}H_{52}NO_7P$	509.3481	6.14	−10	ESI−	−57.37	0.00025[a]
LPC (18:0) sn-1	$C_{26}H_{54}NO_7P$	523.3637	6.19	1.39	ESI+	−55.23	0.0045[a]
LPC (P-18:1) sn-1	$C_{26}H_{52}NO_6P$	505.3532	6.19	−1.98	ESI+	−53.69	0.0068[a]
LPC (19:0) sn-2	$C_{27}H_{56}NO_7P$	537.3790	6.5	−0.43	ESI+	−26.74	0.047
LPC (20:4) sn-2	$C_{28}H_{50}NO_7P$	543.3325	5.38	1.10	ESI+	−45.74	0.012[a]
LPC (22:5) sn-1	$C_{30}H_{52}NO_7P$	569.3481	5.67	−2.18	ESI+	−74.06	0.0034[a]
LPC (22:6) sn-1	$C_{30}H_{50}NO_7P$	567.3325	5.37	0.71	ESI+	−67.46	0.0059[a]
Sphingolipids							
SM (32:1)	$C_{37}H_{75}N_2O_6P$	674.5363	8.02	−2.82	ESI+	−71.75	0.0038[a]
SM (33:1)	$C_{38}H_{77}N_2O_6P$	688.5519	8.42	−2.90	ESI+	−58.25	0.023[a]
SM (34:2)	$C_{39}H_{77}N_2O_6P$	700.5519	8.19	−1.14	ESI+	−53.68	0.015[a]
SM (34:1)	$C_{39}H_{79}N_2O_6P$	702.5675	8.85	2.75	ESI+	−55.33	0.019[a]
PI-Cer (40:1)	$C_{46}H_{90}NO_{11}P$	863.6252	9.45	11.34	ESI+	−77.05	0.013[a]
Sterol lipids							
Glycocholic acid	$C_{26}H_{43}NO_6$	465.309	3.61	1.1	ESI±	(HC)[b]	–
Cholic acid	$C_{24}H_{40}O_5$	408.2876	4.17	−1.1	ESI−	+1053	0.025
Deoxyvitamin D3	$C_{27}H_{44}$	368.3443	10.28	2.44	ESI+	+123.10	0.029[a]
Dihydroxy-oxo-vitamin D3	$C_{27}H_{42}0_4$	430.3083	5.43	−4.65	ESI+	+306.08	0.00002
Trinorvitamin D3 carboxylic acid	$C_{24}H_{36}O_3$	372.2664	4.25	−2.42	ESI+	+1709.64	0.026[a]
Carnitine and derivatives							
Carnitine	$C_7H_{15}NO_3$	161.1051	0.25	2.48	ESI+	−17.68	0.040

Table 3 continued

Name	Compound	Mass (DB)	RT (min)	Mass error (ppm)	DET	Change (%)	*p* value
Oleoylcarnitine	$C_{25}H_{47}NO_4$	425.3504	5.32	−1.87	ESI+	+30.34	0.035
Linoleoyl carnitine	$C_{25}H_{45}NO_4$	423.3348	5.02	−2.05	ESI+	+35.59	0.015
Linoleoyl taurine	$C_{20}H_{37}NO_7P$	387.2439	2.12	4.42	ESI+	−12.57	0.0064
Propanoylcarnitine	$C_{10}H_{19}NO_4$	217.1314	0.26	−0.46	ESI+	+44.42	0.012
Others							
Cytosine	$C_4H_5N_3O$	111.0432	0.27	0	ESI+	+20.28	0.042
Leucyl-proline or isoleucyl-proline	$C_{11}H_{20}N_20_3$	228.1473	0.26	−2.19	ESI+	−16.72	0.0063[a]
Bilirubin	$C_{33}H_{36}N_4O_6$	584.2634	7.84	−0.51	ESI+	−35.30	0.029[a]

Mass (DB), monoisotopic mass recorded in databases; RT (min), retention time; DET, detection mode; Mass error (ppm), difference (in parts per million) between the experimental molecular weight and monoisotopic mass; Change (%), percentage of change of the abundances, calculated as (HC-fed group − Control)/Control; PE, phosphatidylethanolamine; PC, phosphatidylcholine; LPE, lyso-phosphatidylethanolamine; LPC, lyso-phosphatidylcholine; SM, sphingomyelin; PI-Cer, phosphoinositol ceramide. Lipids nomenclature is based on the chemical nomenclature provided by the consortium LIPID Metabolites and Pathways Strategy (LIPID MAPS, http://www.lipidmaps.org)

[a] *p* values corrected by Benjamin Hochberg (FDR correction)

[b] Metabolites identified only in one group (HC-fed group)

Table 4 Differences in plasma metabolites based on GC–MS related to high-cholesterol diet (*p* value <0.05)

Name	Compound	Target ion	RT (min)	Qualifier ion (Q)	CV for QC (%)	Change (%)	*p* value
Cholesterol	$C_{27}H_{46}O$	129	27.47	73, 329, 95	8.99	+54.03	0.00001[a]
Lysine	$C_6H_{14}N_2O_2$	174	17.60	73, 218, 230	38.36	+57.51	0.033
Arachidonic acid	$C_{20}H_{32}O_2$	117	21.69	73, 106, 91	25.65	−34.72	0.028
2-Ketoisocaproic acid	$C_6H_{10}O_3$	73	9.06	73, 200, 89	31.13	−63.14	0.034
Glycine	$C_2H_5NO_2$	174	10.38	174, 73, 147	35.65	+45.56	0.027
D-Galactopyranoside	$C_7H_{14}O_6$	204	18.65	73, 147, 157	10.55	−20.17	0.020
Glycerol	$C_3H_8O_3$	73	9.94	73, 147, 205	9.66	−23.48	JK
Acetoacetate	C_4H_6O3	73	7.92	73,75, 202	40.81	+50.23	JK
Citric acid	$C_6H_8O_7$	73	16.55	73, 273, 142	–	+189.12	JK
Pyranoses	$C_6H_{12}O_6$	73	17.2–17.5	73, 319, 205	–	+147.87	JK
L-Serine	$C_3H_7NO_3$	73	9.75	73, 204, 103	9.75	+47.56	JK
Glyceric acid	$C_3H_6O_4$	73	10.72	147, 73, 66	–	+9.2	JK

RT (min), retention time; CV for QC (%), CV obtained for the same feature within the set of quality control samples; Change (%), percentage of change of the abundances, calculated as (HC-fed group − Control)/Control

Jack–Knife (JK) confidence intervals estimative, 95 % confidence level

[a] *p* values corrected by Benjamin Hochberg (FDR correction)

Fig. 1). Disturbances were not observed, with exception of an increment in the amount of depositions and a reduced apparent diet digestibility, thus assuming an increment in the lipid excretion due to cholesterol overload.

To synthetize the findings in the present study, the main metabolic pathways altered by the HC diet are explained in Fig. 4, and principal metabolites affected on each route are schematically presented, indicating that whether a positive or negative regulation was found.

Cholesterol catabolism addresses bile acid synthesis as the primary pathway affected by the HC feeding. Plasma fingerprinting confirmed the stimulation of the pathways involving cholesterol and bile acid metabolisms, such as circulating cholesterol and some of their primary bile acid and subsequent formation of secondary glycine-conjugated forms, which were found to be significantly up-regulated in the HC group. However, for the correct interpretation of these findings, it has to be considered the likely effect/contribution of the cholate added to the diet in order to increase the cholesterol absorption ratio, in the increased pattern of bile acids secretion. Moreover, it has been suggested that bile acids can trigger the expression of certain genes, through processes like the activation of the FXR-α. The role of this receptor, beyond bile acid homeostasis, has emerged as an important regulator at several levels, including regulatory evidences on the lipid metabolism [32].

Table 5 Differences in plasma metabolites based on CE–MS related to high-cholesterol diet (p value <0.05)

Name	Compound	Mass (DB)	RT (min)	Mass error (ppm)	CV for QC (%)	Change (%)	p value
Acetyl-L-carnitine[a]	$C_9H_{18}NO_4$	204.1235	12.10	−6.8	–	(HC)[c]	–
Propionyl-L-carnitine[a]	$C_{10}H_{19}NO_4$	217.1314	14.20	−0.96	4.59	+35.08	0.031
Arginine[a]	$C_6H_{14}N_4O_2$	174.112	11.64	0.91	1.76	−53.58	0.048
NG,*NG*-dimethyl-L-arginine[a]	$C_8H_{18}N_4O_2$	202.1430	12.37	−6.0	5.78	+23.25	0.079[b]
Kynurenine[a]	$C_{10}H_{12}N_2O_3$	208.0847	15.35	0	7.67	+39.59	0.034
Ornithine[a]	$C_5H_{12}N_2O_2$	132.0898	11.20	−0.56	3.74	+155.36	0.28[b]
Betaine[a]	$C_5H_{11}NO_2$	117.090	17.01	1.68	3.94	+48.91	0.028[b]
Isoputreanine	$C_7H_{16}N_2O_2$	160.1211	11.54	−7.98	3.39	+21.97	0.031[b]
Nx-Acetylspermidine	$C_9H_{21}N_3O$	187.1685	10.47	−3.75	8.59	+29.71	0.0045
Asparagine[a]	$C_4H_8N_2O_3$	132.0534	15.75	−18.87	1.8	+37.05	0.080[b]
Serine[a]	$C_3H_7NO_3$	105.0426	15.18	3.78	0.798	+10.37	0.014
5-Hydroxylysine[a]	$C_6H_{14}N_2O_3$	162.10004	11.72	−2.15	6.35	+11.89	0.030
Histidine[a]	$C_6H_9N_3O_2$	155.0695	11.87	0.62	1.88	+12.66	0.0023
N-methyl-L-histidine[a]	$C_7H_{11}N_3O_2$	169.0850	12.13	0.01	2.42	+25.97	0.017
Cysteine–homocysteine disulfide[a]	$C_7H_{14}N_2O_4S_2$	254.0395	15.55	0.76	1.69	−31.55	0.037
Cytidine[a]	$C_9H_{13}N_3O_5$	243.0854	14.71	−0.39	2.37	+20.65	0.017

Mass (DB), monoisotopic mass recorded in databases; RT (min), retention time; Mass error (ppm), difference (in parts per million) between the experimental molecular weight and monoisotopic mass; CV for QC (%), CV obtained for the same feature within the set of quality control samples; Change (%), percentage of change of the abundances, calculated as (HC-fed group − Control)/Control

[a] Metabolites confirmed by analysis of the standards

[b] p values corrected by Benjamin Hochberg (FDR correction)

[c] Metabolites identified only in one group (HC-fed group)

Table 6 Plasma total cholesterol, HDL cholesterol, LDL cholesterol and triacylglycerides in rats fed the control (C) and high-cholesterol (HC) diets for 7 weeks

	C	HC
Total cholesterol (mg/dL)	83.88 ± 6.86	198.25 ± 10.61*
HDL cholesterol (mg/dL)	60.00 ± 4.94	51.50 ± 3.74
LDL cholesterol (mg/dL)	11.88 ± 0.69	118.63 ± 8.23*
Triacylglycerides (mg/dL)	84.38 ± 6.69	40.50 ± 3.06*

The data are presented as the mean ± SE ($n = 8$ per group)

C control, *HC* high-cholesterol

* ($p < 0.05$) indicates a significant difference between the control and the HC-fed groups (Student's t test)

In addition, some particular functions of cholesterol, like acting as a precursor of vitamin D, or certain transporters mediating the bile acid efflux, may involve spillover routes such as bilirubin excretion [33]. In this regard, metabolites related to vitamin D3 metabolism and its degradation were found to be at higher levels at the HC group too, while bilirubin was detected at lower concentration. Reboul et al. [34] demonstrated that vitamin D and cholesterol, which display a sterol-like structure, may share common absorption pathways. Thus, it could be hypothesized that a simultaneous increase in vitamin D through a major intestinal absorption might also occur in the HC group by stimulation of cholesterol absorption, which was induced when including cholate in the diet of this group. However, the prolonged in time stimulation of the vitamin D3 metabolization might have also lead to depletion in the vitamin D3 levels. According to this statement, it has been recently suggested the relationship between hyperlipidemia and the low values of vitamin D, which may therefore contribute to the development of atherosclerosis [35].

Furthermore, the potential effects of vitamin D as a steroid hormone related to cholesterol are an important issue of discussion since it seems to affect the insulin sensitivity, as well as it is potentially linked to the glucose metabolism via up-regulation of the lipoprotein lipase (LPL) [36]. It has also been found to play an important role in the modulation of the immune inflammation [37].

Therefore, a theoretical postulation about some modifications on the cholesterol and bile acids metabolism would rely on a direct impact on lipid, glucose and energy homeostasis. The present hypercholesterolemic model induced by the HC diet also confirmed the latter.

Besides the steroidal species previously discussed, the most marked metabolic changes in the present study were those involving lipid metabolism, highlighting the glycerophospholipids and sphingolipids species, as well as the free polyunsaturated fatty acids, as the main metabolites

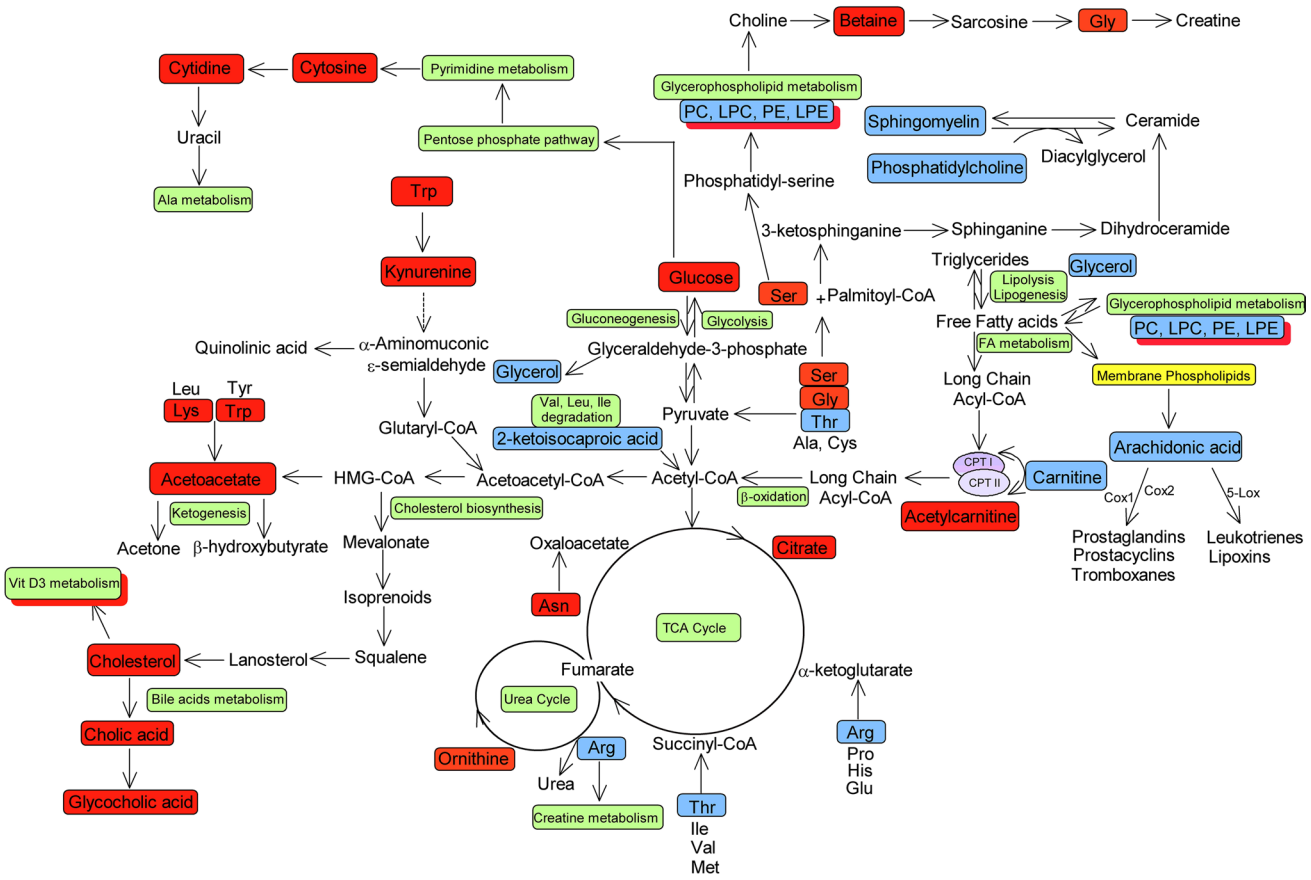


Fig. 4 Schematic representation of the major pathways illustrating the changes due to the hypercholesterolemic diet (HC). *Red-* and *blue-colored boxes* represent significant up-regulated and down-regulated metabolites in the HC-fed group compared to the control, respectively. *5-Lox* 5-Lipoxygenase, *HMG-CoA* 3-hydroxy-methyl-glutaryl-CoA

detected. Among them, phosphatidylethanolamine (PE) and phosphatidylcholine (PC) showed to be predominantly down-regulated. Interestingly, a reduction in various sphingomyelins species was also observed.

PCs are the main membrane-forming phospholipids in mammalian cells, and it was the most abundant specie detected in this study. The removal of one of the fatty acids, through the enzymatic action of a phospholipase A_2 (PLA_2) or by spontaneous hydrolysis, results in the formation of lysophosphatidylcholine (LPC) [38]. Changes in the lecithin-cholesterol acyltransferase (LCAT) activity could also influence plasma LPC levels [39]. Deficitary states in HDL are linked to a decrease in LCAT activity [40, 41]. Nevertheless, no significant change in the HDL concentration of the HC group compared to the control was found, which enabled us to discard such modifications of LCAT as the main cause of the LPC decreased found in the HC group. By contrast, it is well known that the hepatic secretion is a quantitatively important source of plasma LPC [42]. Thus, its depletion in the HC group could be a sign of the possible hepatic inflammation developed in this model.

Recent studies have proved that a reduction in LPC in plasma may be related to inflammatory processes associated with certain diseases and might be used as an indicator for malignant or disease marker [43]. The comparison of LPC between the control and the HC group showed not only a decrease in the total amount of LPC containing saturated (16:0, 17:0, 18:0, 19:0) and monosaturated, polyunsaturated (18:1, 20:4, 22:5, 22:6) chains, but also the implication of specific fatty acids. Their levels in plasma were also related to those of free fatty acids (e.g., arachidonic acid).

Arachidonic acid (AA) is released from PL bilayers in response to different stimuli, and it can be subsequently metabolized through three different enzymatic pathways—cyclooxygenase (COX), lipoxygenase (LOX) and cytochrome (CYP) P450—leading to an important family of regulatory molecules [44, 45]. High levels of AA generally induce an equivalent inflammatory response, since it is the main precursor of eicosanoids in the metabolism. However, some studies show how plasma concentrations of AA are lower under pathological conditions [46], and it

has been suggested that EPA, DHA and AA concentrations cannot be predictive of CVD by themselves [47].

Therefore, the regulation of AA (which was found down-regulated in the HC group compared to the control), as well as other PUFA-containing metabolites found in the present study, must be carefully interpreted, since their change could be due to either a depletion of several enzymatic functions, changes on the modulation of desaturases, or its transformation to other metabolites such as eicosanoids and endocannabinoids, among others [48, 49].

In this context, the transport of fatty acids into the mitochondria for their β-oxidation is a relevant process with a high impact on the energy metabolism. L-carnitine is an essential metabolite, which can be found circulating as free carnitine or acylcarnitines with different lengths [50]. Lower levels of free carnitine and the up-regulation of long-chain acyl fatty acid derivative esters of carnitine (acetylcarnitine, linoleolycarnitine and oleoylcarnitine) were found in this study, and it could be a reflect of an incomplete β-oxidation metabolism in the HC group compared to the control. It has been described that disturbances in the carnitine homeostasis may lead to the accumulation of acylcarnitines and an increased accumulation of acetyl-CoA in target tissues, thus generating the activation of pro-inflammatory pathways, which may cause clinical symptoms implicated in disorders as insulin resistance [51, 52].

In addition, the level of arginine was markedly decreased in the HC group compared to control, suggesting either a low formation of this amino acid due to alterations in the *tricarboxylic acid cycle* (accompanying an impaired mitochondrial function) or its transformation to ornithine, which in turn can be used as precursor for the synthesis of polyamines, proline or glutamate. However, the up-regulation of ornithine (which showed 155 % of change compared to the control group) together with the high levels of some metabolites putatively identified as isoputreanine and acetylspermidine suggests the alteration of both pathways.

Furthermore, the methylation and subsequent proteolysis of protein-incorporated L-arginine residues cause the liberation of methylated compounds such as asymmetric dimethylarginine (ADMA), which inhibits NO bioavailability by competing with L-Arg for binding to NOS, thus compromising the endothelial function [53]. Moreover, elevated ADMA levels (as those reported in this study) have been associated with multiple abnormalities, emphasizing its relation with atherosclerosis, heart failure, chronic kidney disease, diabetes mellitus and insulin resistance [54–60]. Sheen et al. [61] have recently published a review pointing out the relation of ADMA with multiple organ failure based on a model of bile duct ligation in rat, where they have mentioned an increased level in the hepatic protein arginine methyltransferase-1, as well as a decreased dimethylarginine dimethylaminohydrolase expression as a possible cause of ADMA elevation.

Among other routes which were altered after the HC feeding, a singular mention must be done to the kynurenine (KYN) pathway. KYN is the major intermediate product of tryptophan metabolism, and the accumulation of its metabolites is known to be responsible for some pathological conditions, such as sever uremia and its symptoms [62]. Interestingly, our attention must also rely on this mechanism since Pawlak et al. [63] provided insights into the relationship between KYN pathway activation, endothelial dysfunction and atherosclerosis in uraemic patients. This study evidenced an increase in kynurenine in plasma for the HC group, which might alert about the risk that a prolonged in time HC feeding could predispose to the impairment of kidneys functionality.

On the contrary, betaine (an important amino acid conferring protection against renal dysfunction [64] was also identified in this study, and its levels were found to be significantly major in the HC group compared to control. This metabolite results from the oxidation of choline, and it can act as a methyl donor for homocysteine [65]. Nevertheless, the levels of this sulfur-containing amino acid were not significantly modified, but alterations in the methionine and folate cycle were clearly evidenced since higher levels of glycine, serine and other methylated compounds were also confirmed.

It has also been appreciated that hypercholesterolemic rats showed higher levels of cytosine and its nucleoside cytidine in plasma compared to the control rats. Cytidine levels are important since it is not only part of the nucleic acids, but serve as a partial modulator for the pentose phosphate pathway and for the biosynthesis of glycerophospholipids [66].

Conclusions

A wide range of species were identified in plasma and the mapped on their related pathways allowed to create hypotheses for future studies elucidating the mechanism of action underlying the hypercholesterolemia event in Wistar rats. The model describes alterations in lipid energy metabolism and signaling pathways, showing impairments in the β-oxidation and functions of the *tricarboxylic acid cycle.* Bile acids and vitamin D levels were directly influenced by cholesterol overload, while glycerophospholipids showed to be predominantly down-regulated. Among the modification of free fatty acids in plasma, the change in AA as important lipid mediator arouses different hypothesis for its interpretation. Amino acids that play a central role as intermediates in metabolism resulted affected, pointing out the elevation of both glucogenic and ketogenic amino acids. In addition, arginine metabolism was markedly imbalanced and explained by several metabolites, focusing our

attention on ADMA and ornithine changes, so suggesting that they should be closely monitored in hypercholesterolemia. HC feeding stimulated the alteration of tryptophan metabolism at the level of KYN, warning of the risk of developing other important diseases.

Hence, further studies are required to investigate the mechanism of action involved, and the possibilities to revert or ameliorate the negative effects triggered by HC intake, after consumption of other substances and natural products.

Acknowledgments The study was supported by the Spanish Ministry of Science and Innovation [AGL2010-15910 (subprogram ALI)] and the Spanish Ministry of Economy and Competitiveness (CTQ2014-55279-R). The following projects are also acknowledged: Program Consolider-Ingenio 2010, FUN-C-FOOD, CSD2007-00063 (Spanish Ministry of Science and Innovation), and ALIBIRD, S2009/AGR-1469 (Comunidad de Madrid).

Conflict of interest The authors declare no conflict of interest.

References

1. Nichols M, Townsend N, Scarborough P, Rayner M (2013) Cardiovascular disease in Europe: epidemiological update. Eur Heart J 34:3028–3034
2. Artham SM, Lavie CJ, De Schutter A, Ventura HO, Milani RV (2011) Obesity, age, and cardiac risk. Curr Cardiovasc Risk Rep 5:128–137
3. Sherzai A, Heim LT, Boothby C, Sherzai AD (2012) Stroke, food groups, and dietary patterns: a systematic review. Nutr Rev 70:423–435
4. Andersen CJ, Fernandez ML (2013) Dietary strategies to reduce metabolic syndrome. Rev Endocr Metab Disord 14:241–254
5. van Baak MA (2013) Nutrition as a link between obesity and cardiovascular disease: how can we stop the obesity epidemic? Thromb Haemost 110:689–696
6. Grosso G, Mistretta A, Frigiola A, Gruttadauria S, Biondi A, Basile F, Vitaglione P, D'Orazio N, Galvano F (2014) Mediterranean diet and cardiovascular risk factors: a systematic review. Crit Rev Food Sci Nutr 54:593–610
7. Nascimento AR, Machado M, De Jesus N, Gomes F, Lessa MA, Bonomo IT, Tibiriçá E (2013) Structural and functional microvascular alterations in a rat model of metabolic syndrome induced by a high-fat diet. Obesity 21:2046–2054
8. McEvoy CT, Neville CE, Temple NJ, Woodside JV (2014) Effect of diet on vascular health. Rev Clin Gerontol 24:25–40
9. Neuhofer A, Wernly B, Leitner L, Sarabi A, Sommer NG, Staffler G, Zeyda M, Stulnig TM (2014) An accelerated mouse model for atherosclerosis and adipose tissue inflammation. Cardiovasc Diabetol 13:23
10. Mortensen A, Sorensen IK, Wilde C, Dragoni S, Mullerová D, Toussaint O, Zloch Z, Sgaragli G, Ovesná J (2008) Biological models for phytochemical research: from cell to human organism. Br J Nutr 99:ES118–ES126
11. Rideout TC, Harding SV, Jones PJH, Fan MZ (2008) Guar gum and similar soluble fibers in the regulation of cholesterol metabolism: current understandings and future research priorities. Vasc Health Risk Manag 4:1023–1033
12. Nørskov NP, Hedemann MS, Lærke HN, Knudsen KEB (2013) Multicompartmental nontargeted LC–MS metabolomics: explorative study on the metabolic responses of rye fiber versus refined wheat fiber intake in plasma and urine of hypercholesterolemic pigs. J Proteome Res 12:2818–2832
13. Hanhineva K, Barri T, Kolehmainen M, Pekkinen J, Pihlajamäki J, Vesterbacka A, Solano-Aguilar G, Mykkänen H, Dragsted LO, Urban JF Jr et al (2013) Comparative nontargeted profiling of metabolic changes in tissues and biofluids in high-fat diet-fed Ossabaw pig. J Proteome Res 12:3980–3992
14. Ramprasath VR, Jones PJH, Buckley DD, Woollett LA, Heubi JE (2013) Effect of dietary sphingomyelin on absorption and fractional synthetic rate of cholesterol and serum lipid profile in humans. Lipids Health Dis 12:125
15. He W-S, Wang M-G, Pan X-X, Li J-J, Jia C-S, Zhang X-M, Feng B (2013) Role of plant stanol derivatives in the modulation of cholesterol metabolism and liver gene expression in mice. Food Chem 140:9–16
16. Shulaev V (2006) Metabolomics technology and bioinformatics. Brief Bioinform 7:128–139
17. Armitage EG, Rupérez FJ, Barbas C (2013) Metabolomics of diet-related diseases using mass spectrometry. Trac-Trends Anal Chem 52:61–73
18. Brennan L (2013) Metabolomics in nutrition research: current status and perspectives. Biochem Soc Trans 41:670–673
19. Kouskoumvekaki I, Panagiotou G (2011) Navigating the human metabolome for biomarker identification and design of pharmaceutical molecules. J Biomed Biotechnol Article ID 525497
20. Ciborowski M, Ruperez JF, Martinez-Alcazar MP, Angulo S, Radziwon P, Olszanski R, Kloczko J, Barbas C (2010) Metabolomic approach with LC-MS reveals significant effect of pressure on diver's plasma. J Proteome Res 9:4131–4137
21. Vallejo M, García A, Tunon J, Garcia-Martinez D, Angulo S, Martin-Ventura JL, Blanco-Colio LM, Almeida P, Egido J, Barbas C (2009) Plasma fingerprinting with GC–MS in acute coronary syndrome. Anal Bioanal Chem 394:1517–1524
22. Naz S, García A, Rusak M, Barbas C (2013) Method development and validation for rat serum fingerprinting with CE–MS: application to ventilator-induced-lung-injury study. Anal Bioanal Chem 405:4849–4858
23. Gika HG, Macpherson E, Theodoridis GA, Wilson ID (2008) Evaluation of the repeatability of ultra-performance liquid chromatography–TOF–MS for global metabolic profiling of human urine samples. J Chromatogr B 871:299–305
24. García A, Barbas C (2011) Gas chromatography–mass spectrometry (GC–MS)-based metabolomics. Methods Mol Biol 708:191–204
25. Westerhuis JA, Hoefsloot HCJ, Smit S, Vis DJ, Smilde AK, van Velzen EJJ, van Duijnhoven JPM, van Dorsten FA (2008) Assessment of PLSDA cross validation. Metabolomics 4:81–89
26. Llorach R, Garcia-Aloy M, Tulipani S, Vazquez-Fresno R, Andres-Lacueva C (2012) Nutrimetabolomic strategies to develop new biomarkers of intake and health effects. J Agric Food Chem 60:8797–8808
27. Rezzi S, Collino S, Goulet L, Martin F-P (2013) Metabonomic approaches to nutrient metabolism and future molecular nutrition. Trac-Trends Anal Chem 52:112–119
28. Tajima R, Kodama S, Hirata M, Horikawa C, Fujihara K, Yachi Y, Yoshizawa S, Iida KT, Sone H (2014) High cholesterol intake is associated with elevated risk of type 2 diabetes mellitus—a meta-analysis. Clin Nutr. doi:10.1016/j.clnu.2014.03.001
29. Yasutake K, Kohjima M, Kotoh K, Nakashima M, Nakamuta M, Enjoji M (2014) Dietary habits and behaviors associated with nonalcoholic fatty liver disease. World J Gastroenterol 20:1756–1767
30. Gylling H (2014) Clinical utility of serum markers of cholesterol absorption and synthesis. Curr Opin Lipidol 25:207–212
31. McNamara DJ (2000) Dietary cholesterol and atherosclerosis. Biochim Biophys Acta Mol Cell Biol Lipids 1529:310–320

32. Staels B, Fonseca VA (2009) Bile acids and metabolic regulation: mechanisms and clinical responses to bile acid sequestration. Diabetes Care 32:S237–S245
33. Thomas C, Pellicciari R, Pruzanski M, Auwerx J, Schoonjans K (2008) Targeting bile-acid signaling for metabolic diseases. Nat Rev Drug Discov 7:678–693
34. Reboul E, Goncalves A, Comera C, Bott R, Nowicki M, Landrier J-F, Jourdheuil-Rahmani D, Dufour C, Collet X, Borel P (2011) Vitamin D intestinal absorption is not a simple passive diffusion: evidences for involvement of cholesterol transporters. Mol Nutr Food Res 55:691–702
35. Miñambres I, Sánchez-Quesada JL, Sánchez-Hernández J, Rodríguez J, De Leiva A, Pérez A (2014) Vitamin D concentrations in familial combined hyperlipidemia: effects of lipid lowering treatment. Diabetol Metab Syndr 6: Article number 7
36. Huang Y, Li X, Wang M, Ning H, Lima A, Li Y, Sun C (2013) Lipoprotein lipase links vitamin D, insulin resistance, and type 2 diabetes: a cross-sectional epidemiological study. Cardiovasc Diabetol 12: Article number 17
37. Yin K, Agrawal DK (2014) Vitamin D and inflammatory diseases. J Inflamm Res 7:69–87
38. D'Arrigo P, Servi S (2010) Synthesis of lysophospholipids. Molecules 15:1354–1377
39. Goyal J, Wang K, Liu M, Subbaiah PV (1997) Novel function of lecithin–cholesterol acyltransferase: hydrolysis of oxidized polar phospholipids generated during lipoprotein oxidation. J Biol Chem 272:16231–16239
40. Calabresi L, Simonelli S, Conca P, Busnach G, Cabibbe M, Gesualdo L, Gigante M, Penco S, Veglia F, Franceschini G (2014) Acquired lecithin:cholesterol acyltransferase deficiency as a major factor in lowering plasma HDL levels in chronic kidney disease. J Intern Med. doi:10.1111/joim.12290
41. Schaefer EJ, Anthanont P, Asztalos BF (2014) High-density lipoprotein metabolism, composition, function, and deficiency. Curr Opin Lipidol 25:194–199
42. Sekas G, Patton GM, Lincoln EC, Robins SJ (1985) Origin of plasma lysophosphatidylcholine: evidence for direct hepatic secretion in the rat. J Lab Clin Med 105:190–194
43. Taylor LA, Arends J, Hodina AK, Unger K, Massing U (2007) Plasma lysophosphatidylcholine concentration is decreased in cancer patients with weight loss and activated inflammatory status. Lipids Health Dis 6:17
44. Spector AA (2009) Arachidonic acid cytochrome P450 epoxygenase pathway. J Lipid Res 50:S52–S56
45. Khanapure SP, Garvey DS, Janero DR, Letts LG (2007) Eicosanoids in inflammation: biosynthesis, pharmacology, and therapeutic frontiers. Curr Top Med Chem 7:311–340
46. Das UN (2013) Arachidonic acid and lipoxin A_4 as possible endogenous anti-diabetic molecules. Prostaglandins Leukot Essent Fatty Acids 88:201–210
47. Shoji T, Kakiya R, Hayashi T, Tsujimoto Y, Sonoda M, Shima H, Mori K, Fukumoto S, Tahara H, Shioi A et al (2013) Serum n-3 and n-6 polyunsaturated fatty acid profile as an independent predictor of cardiovascular events in hemodialysis patients. Am J Kidney Dis 62:568–576
48. Astudillo AM, Balgoma D, Balboa MA, Balsinde J (2012) Dynamics of arachidonic acid mobilization by inflammatory cells. Biochim Biophys Acta Mol Cell Biol Lipids 1821:249–256
49. Nakamura MT, Nara TY (2004) Structure, function, and dietary regulation of Delta 6, Delta 5, and Delta 9 desaturases. Annu Rev Nutr 24:345–376
50. Kocsis K, Knapp L, Gellért L, Oláh G, Kis Z, Takakuwa H, Iwamori N, Ono E, Toldi J, Farkas T (2014) Acetyl-l-carnitine normalizes the impaired long-term potentiation and spine density in a rat model of global ischemia. Neurosciences 269:265–272
51. Luo T, Li J, Li L, Yang B, Liu C, Zheng Q, Jin B, Chen Z, Li K, Zhang X, Zhang J (2013) A study on the efficacy and safety assessment of propionyl-L-carnitine tablets in treatment of intermittent claudication. Thromb Res 132:427–432
52. Schooneman MG, Vaz FM, Houten SM, Soeters MR (2013) Acylcarnitines: reflecting or inflicting insulin resistance? Diabetes 62:1–8
53. Cardounel AJ, Cui H, Samouilov A, Johnson W, Kearns P, Tsai AL, Berka V, Zweier JL (2007) Evidence for the pathophysiological role of endogenous methylarginines in regulation of endothelial NO production and vascular function. J Biol Chem 282:879–887
54. Cooke JP (2000) Does ADMA cause endothelial dysfunction? Arterioscler Thromb Vasc Biol 20:2032–2037
55. Cooke JP (2005) ADMA: its role in vascular disease. Vasc Med 10:S11–S17
56. Laleman W, Omasta A, van de Casteele M, Zeegers M, Vander Elst I, Van Landeghem L, Severi T, van Pelt J, Roskams T, Fevery J, Nevens F (2005) A role for asymmetric dimethylarginine in the pathophysiology of portal hypertension in rats with biliary cirrhosis. Hepatology 42:1382–1390
57. Baylis C (2006) Arginine, arginine analogs and nitric oxide production in chronic kidney disease. Nat Clin Pract Nephrol 2:209–220
58. Perticone F, Sciacqua A, Maio R, Perticone M, Galiano Leone G, Bruni R, Di Cello S, Pascale A, Talarico G, Greco L, Andreozzi F, Sesti G (2010) Endothelial dysfunction, ADMA and insulin resistance in essential hypertension. Int J Cardiol 142:236–241
59. Celik M, Cerrah S, Arabul M, Akalin A (2014) Relation of asymmetric dimethylarginine levels to macrovascular disease and inflammation markers in type 2 diabetic patients. J Diabetes Res Article number 139215
60. Nishiyama Y, Otsuka T, Ueda M, Inagaki H, Muraga K, Abe A, Kawada T, Katayama Y (2014) Asymmetric dimethylarginine is related to the predicted stroke risk in middle-aged Japanese men. J Neurol Sci 338:87–91
61. Sheen J-M, Chen Y-C, Tain Y-L, Huang L-T (2014) Increased circulatory asymmetric dimethylarginine and multiple organ failure: bile duct ligation in rat as a model. Int J Mol Sci 15:3989–4006
62. Pawlak D, Tankiewicz A, Buczko W (2001) Kynurenine and its metabolites in the rat with experimental renal insufficiency. J Physio Pharmacol 52:755–766
63. Pawlak K, Myśliwiec M, Pawlak D (2010) Kynurenine pathway—a new link between endothelial dysfunction and carotid atherosclerosis in chronic kidney disease patients. Adv Med Sci 55:196–203
64. Fan C-Y, Wang M-X, Ge C-X, Wang X, Li J-M, Kong L-D (2014) Betaine supplementation protects against high-fructose-induced renal injury in rats. J Nutr Biochem 25:353–362
65. Deminice R, Troncon F, Jordao AA (2013) Methionine and methylation balance: pathways for the production and removal of homocysteine. In: Deminice R, Rosa FR, Jordao AA, Snegursky A (eds) Methionine: biosynthesis, chemical structure and toxicity. Nova Science Publishers, Hauppauge, pp 9–25
66. Tozzi MG, Camici M, Mascia L, Sgarrella F, Ipata PL (2006) Pentose phosphates in nucleoside interconversion and catabolism. FEBS J 273:1089–1101